External and Internal Cloud Condensation Nuclei (CCN) Mixtures: Controlled Laboratory Studies of Varying Mixing States.

Diep Vu[1,2,§], Shaokai Gao[1,♦], Tyler Berte[1,2], Mary Kacarab[1,2], Qi Yao[4], Kambiz Vafai[3] and Akua Asa-Awuku[1,2,4,*]

1.*Department of Chemical and Environmental Engineering, Bourns College of Engineering, University of California, Riverside, CA 92521, USA

2.*Bourns College of Engineering, Center for Environmental Research and Technology (CE-CERT), Riverside, CA 92507, USA

3. Department of Mechanical Engineering, Bourns College of Engineering, University of California, Riverside, CA 92521, USA

4.*Department of Chemical and Biomolecular Engineering, A. James Clark School of Engineering, University of Maryland, College Park, MD 20742.

§. Currently at Ford Motor Company, Research & Innovation Center Dearborn, MI 48124, USA

♦. Currently at Phillip 66 Research Center, Research and Development, Bartlesville, OK 74004, USA

Correspondence to: A. Asa-Awuku (asaawuku@umd.edu)

Abstract

Changes in aerosol chemical mixtures modify cloud condensation nuclei (CCN) activity. Previous studies have developed CCN models and validated changes in external and internal mixing state with ambient field data. Here, we develop an experimental method to test and validate the CCN activation of known aerosol chemical composition with multicomponent mixtures and varying mixing states. CCN activation curves consisting of one or more activation points is presented. Specifically, simplified two component systems of varying hygroscopicity were generated under internal, external, and transitional mixing conditions. κ-Köhler theory predictions were calculated

for different organic and inorganic mixtures and compared to experimentally derived kappa values and respective mixing states. This work employs novel experimental methods to provide information on the shifts in CCN activation data due to external to internal particle mixing from controlled laboratory sources. Results show that activation curves consisting of single and double activation points are consistent with internal and external mixtures, respectively. In addition, the height of the plateau at the activation points are reflective of the externally mixed concentration in the mixture. The presence of a plateau indicates that CCN activation curves consisting of multiple inflection points are externally mixed aerosols of varying water-uptake properties. The plateau disappears when mixing is promoted in the flow tube. At the end of the flow tube experiment, the aerosol are internally mixed and the CCN activated fraction data can be fit with a single sigmoidal curve. The technique to mimic external to internally mixed aerosol is applied to non-hygroscopic carbonaceous aerosol with organic and inorganic components. To our knowledge, this work is the first to show controlled CCN activation of mixed non-hygroscopic soot with hygroscopic material as the aerosol population transitions from external to internally mixed states in laboratory conditions. Results confirm that CCN activation analysis methods used here and in ambient data sets are robust and may be used to infer the mixing state of complex aerosol compositions of unknown origin.

1. Introduction

Atmospheric cloud condensation nuclei (CCN) are comprised of complex mixtures of organic and inorganic compounds. The chemical and physical diversity present in complex mixtures can significantly complicate the quantification of aerosol-cloud interactions, thereby making it difficult to predict CCN activity (e.g., Riemer et al., 2019). In this work, we define mixtures and the aerosol mixing state as the chemical diversity across an aerosol distribution. Knowledge of the mixing state and the chemical composition can greatly improve CCN predictions and has been the focus of several studies (e.g., but not limited to (Bilde and Svenningsson 2004; Abbatt et al. 2005; Henning et al. 2005; Svenningsson et al. 2006; King et al. 2007; Cubison et al. 2008; Kuwata and Kondo 2008; Zaveri et al. 2010; Su et al. 2010; Wang et al. 2010; Spracklen et al. 2011; Ervens et al. 2010; Asa-Awuku et al. 2011; Lance et al. 2012; Liu et al. 2013; Jurányi et al. 2013; Paramonov et al. 2013; Padró et al. 2012; Moore et al. 2012; Meng et al. 2014; Bhattu and Tripathi 2015; Almeida et al. 2014; Schill et al. 2015; Crosbie et al. 2015; Che

et al. 2016; Ching et al. 2016; Mallet et al. 2017; Sánchez Gácita et al. 2017; Cai et al. 2018; Schmale et al. 2018; Mahish et al. 2018; Kim et al. 2018; Chen et al. 2019; Stevens and Dastoor 2019)

It is well accepted that the water content and the point of activation is dependent on more factors than just the supersaturation and dry diameter for CCN active aerosols (Dusek et al., 2006; Petters and Kreidenweis, 2007). The droplet growth and activation of slightly soluble organics can be modified when internally mixed with inorganic salts that readily deliquesce (Cruz et al., 1998; Padró et al., 2002; Svenningsson et al., 2006). Although inorganic salts are well characterized, the quantification of CCN activity is complicated when they are internally mixed with a complex organic. Consequently, simple mixing rules may no longer be appropriate. It has been observed that mixed aerosols can activate at lower supersaturations than their bulk constituents and organic compounds that may not traditionally be considered as water soluble may aid in the formation of a cloud droplet by acting as a surfactant, depressing surface tension, or simply by contributing mass (Cruz et al., 1998; Padró et al., 2007; Svenningsson et al., 2006). In addition, when there is a sufficiently large enough fraction of salt, the slightly soluble core can dissolve before activation, thus lowering the required supersaturation (Sullivan et al., 2009). Thus, the mixing state and extent of mixing can substantially influence CCN activity.

To help minimize the complexity in characterizing aerosol hygroscopic and CCN activation properties, CCN data analysis has traditionally been simplified by assuming that *i)* the aerosols share a similar or uniform hygroscopicity over a particle size distribution, *ii)* the CCN particle size can be described by the electrical mobility diameter, *iii)* CCN consists of few multiply charged aerosols and *iv)* all CCN active aerosols readily dissolve at activation. As a result, a singular sigmoidal fit is commonly applied over the entire CCN activation. However, this method of analysis may not be fully representative of the heterogeneous mixing state occasionally present in the aerosol sample. Thus a CCN mixture refers to the diversity of activated aerosols in the particle population (not the property of an individual particle; i.e., Winkler, 1973; Riemer et al., 2019).

Previous studies have addressed aerosols with singular or internally mixed binary chemical species (e.g. but not limited to, Bilde et al., 2004; Broekhuizen et al., 2004; Petters and Kreidenweis, 2007; Shulman et al., 1996; Sullivan et al., 2009). However, ambient measurements indicate complex aerosol populations consisting of both external and internal mixtures (e.g., but not limited to Ervens et al., 2007; Lance et al., 2012; Moore et al., 2012, Padró et al., 2012). By accounting for the mixing states and extent of mixing in field data sets, CCN concentration predictions can be greatly improved (e.g but not limited to Padró et al., 2012; Wex et al., 2010, Su et a., 2010,

Kuwata and Kondo, 2008). However, dynamic changes in particle mixing states have not been reproduced in the laboratory and subsequent treatment of CCN measurement and analysis have not been readily studied in depth under controlled laboratory conditions.

In this work, we seek to improve the experimental CCN activation analysis techniques of complex mixtures by investigating the influence of mixing state on activation curves with known aerosol composition. Theoretical postulations have already been developed and applied to ambient data sets (e.g., but not limited to, Su et a., 2010, Padró et al., 2012; Bhattu et al., 2016;) but never before has a systematic laboratory experiment controlled and validated the extent of particle heterogeneity for CCN activation. To understand the impact of mixing state on CCN activation, simplified two component mixtures of known compounds with varying hygroscopicities are created under internal, external, and in-between (transition) mixing conditions. In addition, black carbon containing particles (BC) and BC mixing state data is presented. BC is renown for its direct radiative effects yet little is known experimentally about the contributions of BC mixtures to aerosol-cloud interactions at varied mixing states. Previous work investigating the contribution of BC to aerosol-cloud interactions at various mixing states has been studied (e.g., but not limited to Bond et al., 2013 and references therein, Lammel and Novakov 1995; Novakov and Corrigan 1996; Weingartner et al. 1997; Dusek et al. 2006; Kuwata and Kondo 2008; Koehler et al. 2009; McMeeking et al. 2011; Liu et al. 2013; Rojas et al. 2015). However, many of these have been limited more to ambient related field studies and less under controlled laboratory settings. Here, the CCN activation and hygroscopic properties of soot mixed with atmospherically relevant constituents of varying hygroscopicity are investigated under laboratory controlled conditions. This work provides evidence on the differences between inorganic, slightly soluble, and insoluble externally and internally mixed compositions for the uptake of water, and subsequent CCN activity.

2. Experimental Methods

2.1 Aerosol Composition and Sources

The CCN activity of two component aerosol mixtures under internal, external, and combinations of mixing states are explored in this study. The components include very hygroscopic (inorganics), hygroscopic (organic acids), and non-hygroscopic (Black Carbon, BC). For known chemical compositions, a Collison-type atomizer

generated singular-component solutions of ammonium sulfate, ($(NH_4)_2SO_4$, Acros 99.5%), sodium chloride, (NaCl, Acros 99+%) and succinic acid ($C_4H_6O_4$, Acros 99%) and subsequent internal mixture combinations as described in the sections Aerosol Mixing States and Modified Mixing States: External to Internal. Succinic acid, classified as a slightly soluble dicarboxylic acid, (18) $(NH_4)_2SO_4$, and NaCl are all relevant model atmospheric compounds with varying degrees of solubility and hygroscopicity. All atomized solutions were prepared using Millipore© DI water (18 mΩ, TOC ≤ 5 ppb). Atomized wet droplets were dried with silica gel diffusion dryer (as commonly practiced). In addition, we employ a heated column before the diffusion dryer to facilitate the evaporation of water from the wet particles. The implications of the use or absence of a heated column are discussed in the results below.

An AVL Particle Generator (APG), which houses a mini Combustion Aerosol STandard soot generator (miniCAST 6203C, Jing ltd.), was used to generate carbonaceous aerosols. The APG consists of a propane burner followed by a volatile particle remover. The burner was operated at 400°C with a propane and air flow rate of 15 ml per min and 1.0 l per min, respectively. The miniCAST utilized in the APG has been well characterized in previous work (e.g., Pinho et al. 2008; Seong and Boehman 2012; Mamakos et al. 2013; Maricq and Matti Maricq 2014; Durdina et al. 2016; Moore et al. 2014). The soot formed is a mixture of black and oxidized carbon (Moore et al. 2014). The aerosol structures generated by the APG likely consisted of fractal-like agglomerates of non-spherical particles (Moore et al. 2014; Durdina et al., 2016). APG Combustion aerosols are mixed with inorganic and slightly soluble succinic acid and CCN activity is subsequently measured at different supersaturations.

2.2 Aerosol Mixing Methods

Mixing compounds in solution can readily form internal mixtures of aerosol (Gibson et al., 2007; Hameri et al., 2002). Solution mixtures of a highly hygroscopic compound, NaCl, and a slightly hygroscopic compound, succinic acid, are shown. Five aqueous solutions of succinic acid and NaCl with molar ratios of 100:0, 87:13, 69:31, 43:57, 0:100 were aerosolized using a single atomizer, passed through a heated column, dried, and sampled directly into a Scanning Mobility Particle Sizer (SMPS) and CCN Counter (CCNC). Instrument specifications are discussed in section 2.3.

External mixtures were formed via two methods**.** The first and simplest method required two sufficiently dry aerosol streams to mix. Two aerosol streams were joined via a Swagelok® Tee connector. External mixtures were also formed in a flow tube mixing apparatus. As conditions (e.g., but not limited to, residence time, temperature,

pressure, relative humidity) change in a flow tube, it is assumed that the external mixture may transition into an internally mixed aerosol system. A flow tube mixing apparatus was constructed to test this assumption and modify the extent of mixing of multiple components (Fig. 1 & 2).

Figure 1. External and Internal Mixtures with gradual mixing in flow tube

This work shows changes in CCN experimental data and analysis as a result of changes in the extent of mixing. Results of the CCN activation are presented in the Section: Modified Mixing: External to Internal Mixing in the Aerosol Flow Tube. A brief description of the flow tube is provided here. The first aerosol stream is introduced into the flow tube by a ¼ inch stainless steel (SS) tube. The second aerosol stream is also introduced by a ¼ inch SS tube, but is expanded to an outer concentric ¾ inch SS tube using a SS Swagelok tee connection. The two aerosol flows are initially mixed together at the exit of ¼ inch tube and aerosol mixes within the ¾ inch SS tube for an additional 12 inches before entering the quartz tube where it continues to mix. In this study, the pressure and temperature of the flow tube is maintained at ambient conditions. The extent of mixing in the flow tube mixer has been modeled by Computational Fluid Dynamics simulation (CFD - Comsol) to test and improve the aerosol mixing capabilities of the flow tube mixer (Fig. A1). The focus of this work is not the mixing apparatus but the CCN behavior that results from changes in the extent of mixing. It is noted that particle losses likely occur within the flow tube system but do not affect the intrinsic aerosol and CCN properties (activated fractions) presented here.

Figure 2. Example of charge corrected a) a single component activation curve b) a multiple activation curve from an externally mixed/heterogeneous system. The assymptote, η, varies in height and length with the presence of mixed components and their respective hygroscopicities.

2.3 CCN Activity and Chemical Composition: Measurements and Instrumentation

CCN activation is measured with particle sizing and counting instrumentation in parallel with CCN counting instrumentation. This technique is widespread and has been used in numerous publications (e.g., but not limited to,

158 Moore et al., 2010; Padró et al., 2012). The development of a single continuous-flow thermal gradient diffusion
159 column CCN Counter, CCNC (Droplet Measurement Technologies, Inc.) has provided rapid (~1 Hz) and robust
160 CCN data (Lance et al., 2012; Roberts and Nenes, 2005). Aerosols with a S_c lower than the supersaturation in the
161 column activate and form droplets. These droplets are detected and counted using an optical particle counter at the
162 exit of the column.

163 A TSI 3080 Electrostatic Classifier selects and measures aerosol size distributions. Polydisperse aerosol
164 streams are passed through a bi-polar krypton-85 charger and then through a differential mobility analyzer (DMA),
165 where the aerosols are sized according to electrical mobility with a sheath to aerosol flow ratio of 10:1. The
166 monodispersed flow is then split to a CPC and a CCN counter. CN concentrations were measured with a
167 condensation particle counter, CPC (TSI 3772, TSI 3776).

168 The CCNC is operated at 0.5 lpm with a sheath to aerosol flow ratio of 10:1 and is calibrated with $(NH_4)_2SO_4$ to
169 determine the instrument supersaturation (Rose et al., 2008). Operating the CCN in parallel with the CPC allows for
170 the simultaneous measurements of the total CN and CCN of the monodispersed aerosols. By operating the DMA in
171 scanning voltage mode and maintaining a constant column supersaturation, the CCN/CN, or activation ratio, as a
172 function of dry diameter can be obtained for a given supersaturation. These size resolved CCN distributions obtained
173 through scanning mobility CCN analysis (SMCA) are produce CCN activation curves, CCN/CN ratio as a function
174 of particle mobility diameter (Moore et al., 2010). SMCA produces high resolution CCN activation data near the
175 50% efficiency critical diameter every ~ 2 minutes.

176 An Aerodyne high-resolution time-of-flight aerosol mass spectrometer (HR-ToF-AMS) measured the non-
177 refractory bulk composition (DeCarlo et al., 2006). The HR-ToF-AMS was operated in V-mode to track the
178 concentration and vacuum aerodynamic diameter as the aerosol fractions were modified.

179 3. CCN Analytical Method

180 CCN data analysis of single component aerosols, such as AS, are well characterized. The activation of a single
181 known component yields a simple sigmoidal activation curve and is often used for instrument calibration (Fig. 2a).
182 However ambient aerosols generally exist as complex mixtures of organic and inorganic species. CCN data sets
183 from ambient and chamber studies, which consist of these aerosol mixtures, may not show a single sigmoidal

activation curve but instead can exhibit multiple activation curves not associated with doubly charged particles (Fig. 2b).

Sigmoidal fits are applied to the CCN/CN as a function of dry activation diameters for the multicomponent aerosols. Externally mixed aerosol fractions in activation curves have been previously observed in ambient studies by Lance et al. (2013), Moore et al. (2012), and Bougiatioti et al. (2011). For those studies, E was defined as the hygroscopic fraction, and 1-E the non-hygroscopic mixed fraction. For this study the first curve is similarly defined as the hygroscopic externally mixed fraction (EMF) with an asymptote, or plateau of η. The dependence of η varies with the presence of mixed components and their respective hygroscopicities. Thus we evaluate η for controlled compositions and compare how representative they are of the known fractions of mixtures.

A sigmoidal fit through the EMF determines the particle dry diameter of the more hygroscopic species. A second sigmoidal fit is applied to the second activation curve. An example is shown in Fig. 2b for an external mixture of AS and SA. A sigmoid is fit for the more hygroscopic species, AS, and then a second for the less hygroscopic species, SA. The activation diameters are consistent with those expected for the two compounds and agree with Köhler predicted activation values for AS and SA. Doubly charged aerosols are indicated in Figure 2 and are a negligible contribtion to the activation curves.

The supersaturation and critical dry diameter are related via the single parameter hygroscopicity, $\boldsymbol{\kappa}$**,** to describe the CCN activity and to determine the effect of mixing states of multiple components on the supersaturated hygroscopic properties of aerosols. Using the generalized κ-Köhler equations presented by Petters and Kreidenweis (2007 and 2008), droplet growth in the supersaturated regimes for a selected dry diameter can be modeled for an aerosol where the entire particle diameter dissolves at activation.

$$lnS_c = \left(\frac{4A^3\rho_w M_s}{27v\rho_s M_w D_d^3}\right)^{1/2}, \quad where\ A = \frac{4\sigma_{s/a}M_w}{RT\rho_w} \qquad (1)$$

$$\kappa = \frac{4A^3}{27D_d^3 ln^2 S_c} \qquad (2)$$

$\sigma_{s/a}$ is the surface tension, M_w is the molecular weight of water, R the universal gas constant, T is the temperature at activation, and ρ_w is the density of water. Surface tension and density of water were calculated according to temperature dependent parameterizations presented by Seinfeld and Pandis (1998) and Pruppacher and Klett (1997). The surface tension of the solution is assumed to be that of pure water. Traditional Köhler theory is known to work reasonably well for inorganic salts and slightly-soluble and hygroscopic organics like succinic acid.

4. Results and Discussion

4.1 Internal Mixtures

Aerosolized internally mixed solutions exhibit single CCN activation curves for all five compositions of succinic acid and NaCl solutions (Fig. 3a). The activation curve is similar to that of ammonium sulfate in Figure 2a. Multiply charged particles contribute less than 10% to the activated fraction and are assumed to be negligible. A sigmoid that plateaus near one can be applied to describe the CCN activation. As the internal mixture salt fraction increased at a given supersaturation, the single curve was maintained and shifted towards a lower activation diameter, indicative of and consistent with more hygroscopic aerosol. The shifting of the CCN activation sigmoid (left and right) is also expected of internally mixed particles formed via the coagulation of separate particle distributions (Farmer et al., 2015). Using the simple mixing rule, a multicomponent hygroscopicity parameter can be theoretically applied based on the expected kappa values for each individual component hygroscopicity ($\boldsymbol{\kappa_i}$), and the volume fraction of each component (ε_i) (Petters and Kreidenweis (2007).

$$\boldsymbol{\kappa} = \sum_{i} \boldsymbol{\varepsilon_i \kappa_i} \qquad (3)$$

Equation (3) was applied for each mixture. $\boldsymbol{\kappa}$ was calculated and compared to the experimental values (Fig. 3b). These internal mixtures do not strongly follow the simple mixing rule for every mixture and is consistent with the previous work of Shulman et al. (1996) and Padró et al. (2007) who showed that slightly soluble compounds internally mixed with salts resulted in surface tension depression and thus a lower required critical supersaturation. As previously published, accounting for organic surface tension depression could improve kappa-hygroscopicity calculations for internal mixtures. Regardless of surface tension omissions, the single sigmoidal experimental data set is within 20% of theoretical agreement and indicative of a single component or homogeneous internally mixed aerosol population.

Figure 3. a) Activation curves for two component internal mixtures of NaCl and succinic acid (SA) at SS 0.72%. Doubly charged aerosols are present but are all below 0.1 and negligible. **b)** Internally mixed aerosols.

236 Multicomponent hygroscopicity parameter predictions vs. experimentally derived kappa values. Dashed lines
237 indicate 50% uncertainty (1:1.5 and 1.5:1). Data are within 20% uncertainty of the 1:1 line.

238 **4.2 External to Internal Aerosol Mixing Results**

239 Individual single component aqueous solutions of ammonium sulfate (AS), $(NH_4)_2SO_4$, and succinic acid
240 (SA) were aerosolized, dried with an active heated column and silica gel diffusion dryer to produce external
241 mixtures. Data sets yielding multiple activation curves consistent with external mixing were successfully created by
242 *i)* mixing aerosol streams and *ii)* injecting SA and AS-compounds in the flow tube. For this manuscript, we show
243 externally mixed data generated from the use of the mixing flow tube. The direct mixing produces the same external
244 mixed CCN results (not shown). By using aerosols consisting of compounds of significantly different
245 hygroscopicities, and thus different activation diameters, distinct double plateaus for CCN activation can be
246 observed for external mixtures (Fig. 2b). At particle mobility diameters between ~35 and 45 nm there is an
247 asymptote, $\eta \sim 0.6$ (Fig. 4a., 4b., and 4c). It is noted that heated succinic acid particles can evaporate during aerosol
248 generation before CCN measurement; the asymptote in Figure 4 is an indication that multiple components are
249 present in the total aerosol distribution. The activation curves were characteristic of AS and SA, and the measured
250 activation diameters agreed well with Köhler Theory and the single parameter (κ) thermodynamic predictions of
251 droplet activation (Fig. 4a). The external mixture was maintained for an hour as indicated by the separate and stable
252 activation diameters derived from multiple sigmoid analysis. For more than 2-component externally mixed particle
253 distributions, more than two plateaus will be observed. For example, the work of Schill et al. 2015 shows multiple
254 plateaus for a five-component external mixture mimic of ocean spray CCN. If one considers a limiting case of
255 infinite components with distinct varying degrees of hygroscopicity, then the activation curve will be monotonic
256 below 1 and may appear to be representative of an internal mixture; the CCN activation curve will approach the
257 shape of a shallow sigmoidal slope (however not as steep or instantaneous as the ideal step function).
258
259 **Figure 4. External to internal mixtures of a slightly soluble organic aerosol, succinic acid (SA) and inorganic**
260 **ammonium sulfate (AS) aerosol.** The CCNC was operated at a single S_c of 0.8%. Closed symbols are externally
261 mixed. Open symbols are internally mixed. a) The apparent kappa values derived from externally mixed multiple-
262 sigmoid activation data before active heating is turned off (at approximately 3:30 pm) and single sigmoid activation

curves (after 3:30pm) are shown. The two dotted lines indicate the theoretically derived kappa values for succinic acid, κ=0.23, and ammonium sulfate, κ=0.61. b) CCN activation curves exhibit external (with active heating before 3:30 pm) and then transitioning external to internal mixing (after 3:30pm) c) CCN/CN vs. Dry mobility diameter data as a function of time. The asymptote, η, disappears at the by the end of the experiment.

One hour after initial injection into the flow tube, the active heating column was turned off. It should be noted that atomized aerosol continued to be dried through the silica gel diffusion dryers, as is commonly done. The relative humidity after the dryer in both cases is small (< 20%) and thus the activation diameters of very hygroscopic AS calibration aerosol are not affected with or without active heating (Fig. A2). However, as soon as active heating was turned off, particles in the mixing flow tube became more mixed (Figure 4). Thus, it is likely that minute amounts of aerosol water promoted internal mixing and shifted aerosol mixing from external to internal in the mixing flow tube system.

CCN activation curves for the two compounds remained distinct and separate until internal mixing conditions dominated and the multiple CCN activation curves converged into a single curve (Fig. 4b and 4c). Results suggest aerosol water plays a significant factor in mixing and CCN activation. This is consistent with previous work that indicates that the presence of water led to lowered aerosol viscosity and increased diffusivity (Ye et al., 2016). The wetted aerosols can come in contact through diffusion and coalesce to form an internally mixed aerosol. The apparent kappa values from fitting the two individual activation curves for the external part of the mixing experiment and subsequent internal mixing are shown in Fig. 4a.

To help track the change in organic/inorganic fractions during the transition from external to internal, the mixed aerosols were analyzed with a high-resolution time of flight mass spectrometer (HR-Tof-AMS) to provide mass fraction information. The mass size distribution was integrated and normalized for each compound per scan according to the total mass that was measured. The mass size distribution was then converted to number size distribution and the diameters were converted from aerodynamic diameter to electrical mobility diameter. Then for each superstation and fraction, the EMF was calculated between the two respective activation diameters and correlated to the EMF that was determined from SMCA to determine the plateau height (η).

AS fractions measured by the AMS are consistent with the changes SMCA derived η where increases in AS mass fraction increase η. However, the AMS derived AS fraction are slightly lower compared to SMCA (Fig.

5), indicating potential influence on η from other factors. Previous work has shown the presence of highly soluble materials (like AS) can promote CCN activity of organic dominated systems (Asa-Awuku et al., 2011; Fofie et al., 2017). A second flow tube experiment was conducted to test the effect of differing concentrations on plateau heights. The detection efficiency for particles with smaller sizes in the AMS (<50nm) can effect the AS fraction. Thus, the CCNC supersaturation was modified from 0.2 to 1.2% to test the effect of activation diameter on closure (Fig. 6.). Results show good agreement and are within 50% of predictions. Results with distinct CCN activation plateaus, especially of 2-3 distinct hygroscopicities, may be useful for estimating aerosol chemical fractions when other instruments with lower size resolution are not readily available.

Figure 5. Plateau heights derived from AMS data vs. SMCA. Single CCNC Supersaturation. Dashed lines indicate 50% uncertainty (1:1.5 and 1.5:1).

Figure 6. Modifying activation diameters. Plateau heights derived from AMS data vs. SMCA for CCNC Supersaturation from 0.2 to 1.2%. Dashed lines indicate 50% uncertainty (1:1.5 and 1.5:1).

4.3 External and Internal Mixtures of Combustion Aerosol

Combustion aerosol or soot can form external and internal complex aerosol mixtures. Soot is considered insoluble but wettable (e.g., but not limited to Lammel and Novakov 1995; Moore et al. 2014) and the contributions of Black Carbon containing particles to aerosol-cloud interactions at varied mixing states is not well known or understood (Lammel and Novakov 1995; Novakov and Corrigan 1996; Weingartner et al. 1997; Dusek et al. 2006; Kuwata and Kondo 2008; Koehler et al. 2009; Bond et al. 2013; McMeeking et al. 2011; Liu et al. 2013; Rojas et al. 2015). Thus, the ability of black carbon to mix with inorganic and organic compounds and to observe the extent of mixing as they activate as CCN is of great interest.

Prior to investigating the impact of mixing fresh combustion emissions with inorganic and organic aerosols, the CCN activation spectra of soot was measured using combustion aerosol generated from the APG. The aerosol is

likely composed of black carbon and oxidized carbonaceous material (Moore et al. 2014; Durdina et al. 2016). Thus we also refer to carbonaceous aerosol as black carbon mixtures (simply, BC mixtures). The CCN activated fraction data from soot was fit to a singular sigmoidal curve (Fig. 7). There are no plateaus in the activation curve and the single sigmoid fit indicates that the aerosol generated is a homogenous internal mixture. Combustion aerosol activated at a mobility diameter of 133 nm at 2.2% supersaturation. The apparent hygroscopicity of combustion aerosol was κ=0.001, and is consistent with the order of magnitude and kappa values reported for fresh combustion aerosol from diesel engine sources (Fig. 7) (Vu et al., 2015; Moore et al. 2014). It is noted that the apparent hygroscopicity is defined by the electrical mobility diameter that assumes particles are spherical.

Figure 7. Combustion aerosol activation curve (SS 2.2%, $d_{p,50}$=133nm, $\boldsymbol{\kappa}$=0.001)

Next, the influence of modifying externally mixed hygroscopic aerosol fractions with non-hygroscopic BC mixtures was observed. Soot was externally mixed with various concentrations of AS and NaCl in two separate experiments. For each BC mixture, combustion aerosol was introduced to the flow tube and atomized inorganic and organic aerosol (dried with a heated column and silica gel diffusion dryers) was injected. The concentration of inorganic in the flow tube was slowly increased to modify the contribution of soluble material. The CCN counter supersaturation was decreased to 1.1% to observe the impact of the more hygroscopic compounds in the BC mixture.

Figure 8 shows the CCN activation of external mixtures of BC with AS and NaCl at S_c = 1.1%. The initial combustion size distribution at the start of the experiment and the modified CCN activation fractions of the aerosol mixtures are presented. The shape of the activation curve provides insight about the sizes of very hygroscopic and non-hygroscopic species. At S_c = 1.1% BC particles, with κ = 0.001, will not theoretically activate below 250 nm and the contribution of externally mixed BC in the size range shown does not contribute much (if any) CCN. The normalized size distribution data show that there are few BC-like particles at small sizes (<50 nm), the majority of particles in this range are inorganic. Thus for both the AS and NaCl external mixtures, the activation diameters derived from a singular fit were consistent with the expected d_{p50} < 50 nm of the respective inorganic salts. Specifically at S_c=1.1%, AS and NaCl particles activated at 25 and 19 nm respectively (congruent with theoretical dp50 at 24.8 and 19.0 nm) At the larger sizes (> inorganic d_{p50}), the BC mixture concentration increased and the

CCN/CN was depressed. The combustion aerosol alone is not CCN active at this S_c or size and the depressions are reflective of the non-hygroscopic combustion aerosol fraction in the aerosol sample. Notably, plateaus are dynamic. As the concentration of inorganic salts increase, the increased activated fraction is reflected in the CCN spectra; the plateau heights increase with increasing hygroscopic concentrations. In these particular externally mixed experiments, the initial CCN/CN plateau can be as large as one, subsequently decrease, and then will likely increase to one after the BC critical diameters are reached. BC externally mixed with very hygroscopic material is more CCN active than the soot alone.

Figure 8. Combustion aerosols externally mixed with inorganics a) NaCl externally mixed with concentrations modified from 51% to 85% over the course of 60 min b) AS externally mixed with concentrations from 41% to 86% over a course of 75 min. Cross symbols represent the initial size distribution of the combustion aerosol.

Succinic acid (SA) was mixed with combustion aerosol to investigate the external to internal mixing and transition of slightly hygroscopic organic with non-hygroscopic insoluble but wettable aerosols. The laboratory system mimics observed increases in SOA mass fractions on combustion aerosols during atmospheric aging. The SA was introduced to the flow tube at various concentrations, followed by the combustion aerosol from the APG, under dry externally mixed conditions and bimodal size distribution peaks were observed (Figure 9).

The normalized size distributions of the aerosol leaving the flow tube are presented. The initial soot size distribution is similar to those presented in Figure 8. Assuming the first of the two peaks is SA, and the second is a mixture of the combustion aerosol and SA, the initial point of activation agrees with that of succinic acid where SA aerosols all activate. After a mobility diameter, $dp > 50$ nm, the concentration of combustion aerosol in the mixture increases and the CCN/CN ratio is < 0.2, indicative of a lower SA concentration relative to the non-activated BC concentration.

To induce internal mixing, active heating was again turned off for the atomized aerosol source. Again, internal mixing was promoted and the multiple activation curves converge into a single sigmoid for the BC and SA system.

This is consistent with the AS/SA experiment and previous work that showed a strong influence of insoluble compounds on activation when internally mixed with a more soluble compound. (9) With continued mixing, a shift to larger activation diameters was observed towards the end of the experiment (scan 93) and there was a slight depression in the plateau of the CCN spectra.

The data suggests that only a small amount of soluble inorganic and organic material is required to make the soot more active than that observed alone, especially as the aerosol becomes more internally mixed.

Figure 9. a) Time series of CCN/CN activated fractions of Succinic Acid (SA) and combustion aerosol (BC) mixture in flow tube. b) The CCN/CN activated fraction (closed triangles) of SA and BC mixtures for particle distribution scans 24, 45, 54, 73, and 94. Aerosol water is introduced at ~ scan 70 to promote internal mixing. Cross symbols show the particle size distribution mixed aerosol.

5. Conclusion

Results confirm that the experimental CCN activation curves of aerosol provide insight into to the type of mixing (e.g. internal vs. external) and the various levels of hygroscopicities that are chemically representative. Modifications in the concentrations of externally mixed non-hygroscopic aerosols are reflective of the CCN activated concentrations. This is consistent with CCN spectra observed in ambient studies, which have attributed observations in CCN activation plateau heights less than one to the contributions of externally mixed and inactivated (typically non-hygrosocopic black carbon) aerosols. This work adds to the existing body of CCN literature and demonstrates that the transition from external to internal mixtures can be mimicked in controlled laboratory experiments and observed in CCN data. If one accounts for multiple-sigmoid analysis in experimental CCN activation data, the CCN behavior of known hygroscopic compound mixtures (e.g., ammonium sulfate, sodium chloride, succinic acid) agrees well with traditional Köhler theory. However, more work is needed to explore mixtures of hygroscopic material particularly with wettable and non-hygroscopic aerosol. Here, as the non-

hygroscopic combustion aerosol becomes internally mixed with the inorganic and organic material, the CCN activity of the combustion aerosol is modified. The data here, with recent publications (Altaf et al., 2018; Ye at al., 2016), suggest that aerosol water is a significant factor in promoting mixing and can be used to modify mixing states. To our knowledge, the technique provided here is the first to show aerosol population transitions from external to internally mixed states in a laboratory environment and thus the technique can be applied to understand additional aerosol properties (e.g., optical, gas-phase uptake, subsaturated droplet growth, etc.) of known compounds that can modify particle mixing states. The aerosols studied here maintained an external mixture under dry conditions; CCN activation curves plateaued and remained constant. However, turning off the heater promoted internal mixing and the activation curves were observed to converge. These experiments with known compounds validate that the aerosol mixing state can be observed in CCN activation data and can be applied to aerosol data sets to understand the extent of mixing. The results confirm that CCN counters and CCN analysis should be used in future studies to quantify the extent of mixing of ambient particles. The results are critical to understanding other factors important to the direct and indirect radiative contributions of atmospheric particles.

Acknowledgments

This work was supported by the University of California Transportation Center and the U.S. Environmental Protection Agency (EPA) grant number 83504001. Diep Vu thanks the U.S. Environmental Protection Agency (EPA) STAR Fellowship Assistance Agreement no. FP-91751101. EPA 83504001 was fundamental for the development of the mixing flow tube apparatus. Additionally, AA would like to thank the National Science Foundation (NSF) proposal 1151893. The contents of this paper are solely the responsibility of the grantee and do not necessarily represent the official views of the EPA or NSF. Further, the EPA and NSF do not endorse the purchase of any commercial products or services mentioned in the publication. In addition the authors would like to acknowledge Desiree Smith, Drs. Kent Johnson and Heejung Jung for their role in the acquisition of APG and access to controlled BC measurement and Dr Jeffrey Pierce for advice on CCN models.

Data availability.

The data and figures will be made available upon request from authors Diep Vu and corresponding author Akua Asa-Awuku.

Author contributions.

SG built the mixing flow tube device used in the experiments. KV developed fluid models to characterize the flow of particles in the instrument. TB and MB assisted with experimental measurements presented. DV conducted measurements, analysis and contributed to the writing of the manuscript. AAA developed the concept for this work and contributed to the analysis and writing of the manuscript.

Competing interests.

The authors declare that they have no conflict of interest.

References

1. Abbatt, J. P. D., Broekhuizen, K., and Kumar, P. P.: Cloud condensation nucleus activity of internally mixed ammonium sulfate/organic acid aerosol particles, Atmos. Environ., 39, 4767-4778, 2005.
2. Altaf, M. B. Dutcher, D D. Raymond,T. M and Freedman, M. A.: Effect of Particle Morphology on Cloud Condensation Nuclei Activity, ACS Earth and Space Chem., 10.1021/acsearthspacechem.7b00146. 2018.
3. Asa-Awuku, A., Moore, R., Nenes, A., Bahreini, R., Brock, C. A., Middlebrook, A., Holloway, J., Ryerson, T., Jimenez, J., DeCarlo, P., Hecobian, A., Weber, R., Tanner, D., Stickel, R., and Huey L. G., 'Airborne Cloud Condensation Nuclei Measurements during the 2006 Texas Air Quality Study, J. Geophys. Res., 116, doi:10.1029/2010JD014874. 2011.
4. Bhattu, D., Tripathi, S. N., and Chakraborty, A.: Deriving aerosol hygroscopic mixing state from size-resolved CCN activity and HR-ToF-AMS measurements, Atmos. Environ., 142, 57-70, 2016.
5. Bilde, M. and Svenningsson, B.: CCN activation of slightly soluble organics: The importance of small amounts of inorganic salt and particle phase, Tellus, 56B, 128–134, 2004.
6. Bond, T. C., Doherty, S. J., Fahey, D. W., Forster, P. M., Berntsen, T., DeAngelo, B. J., Flanner, M. G., Ghan, S., Karcher, B., Koch, D., Kinne, S., Kondo, Y., Quinn, P. K., Sarofim, M. C., Schultz, M. G., Schulz, M., Venkataraman, C., Zhang, H., Zhang, S., Bellouin, N., Guttikunda, S. K., Hopke, P. K., Jacobson, M. Z., Kaiser, J. W., Klimont, Z., Lohmann, U., Schwarz, J. P., Shindell, D., Storelvmo, T., Warren, S. G., and Zender, C. S.: Bounding the role of black carbon in the climate system: A scientific assessment. J. Geophys. Res., 118, 5380-5552, 2013.
7. Bougiatioti, A., Nenes, A., Fountoukis, C., Kalivitis, N., Pandis, S. N., and Mihalopoulos, N.: Size-resolved CCN distributions and activation kinetics of aged continental and marine aerosol, Atmos. Chem. Phys., 11, 8791-8808, doi:10.5194/acp-11-8791-2011, 2011.
8. Broekhuizen, K., Kumar, P. P., and Abbatt, J. P. D.: Partially soluble organics as cloud condensation nuclei: Role of trace soluble and surface active species, Geophys. Res. Lett., 31, doi:10.1029/2003GL018203, 2004.

9. Cai, M., Tan, H., Chan, C. K., Qin, Y., Xu, H., Li, F., Schurman, M. I., Liu, L. and Zhao, J.: The size-resolved cloud condensation nuclei (CCN) activity and its prediction based on aerosol hygroscopicity and composition in the Pearl Delta River (PRD) region during wintertime 2014, Atmos. Chem. Phys., 18(22), 16419–16437, 2018.
10. Chen, L., Li, Q., Wu, D., Sun, H., Wei, Y., Ding, X., Chen, H., Cheng, T. and Chen, J.: Size distribution and chemical composition of primary particles emitted during open biomass burning processes: Impacts on cloud condensation nuclei activation, Sci. Total Environ., 674, 179–188, 2019.
11. Ching, J., Riemer, N. and West, M.: Black carbon mixing state impacts on cloud microphysical properties: Effects of aerosol plume and environmental conditions, J. Geophys. Res.,-Atmos, 121(10), 5990–6013, 2016.
12. Crosbie, E., Youn, J.-S., Balch, B., Wonaschütz, A., Shingler, T., Wang, Z., Conant, W. C., Betterton, E. A. and Sorooshian, A.: On the competition among aerosol number, size and composition in predicting CCN variability: a multi-annual field study in an urbanized desert, Atmos. Chem. Phys., 15, 6943–6958, 2015.
13. Cruz, C. N. and Pandis, S. N.: The effect of organic coatings on the cloud condensation nuclei activation of inorganic atmospheric aerosol, J. Geophys. Res., 103, 13111-13123, 1998.
14. Cubison, M. J., Ervens, B., Feingold, G., Docherty, K. S., Ulbrich, I. M., Shields, L., Prather, K., Hering, S. and Jimenez, J. L.: The influence of chemical composition and mixing state of Los Angeles urban aerosol on CCN number and cloud properties, Atmos. Chem. Phys., 8(18), 5649–5667, 2008.
15. DeCarlo, P. F., Kimmel, J. R., Trimborn, A., H., Northway, M. J., Jayne, J. T., Aiken, A. C., Gonin, M., Fuhrer, K., Horvath II, T., Docherty, K. S., Worsnop, D. R., Jimenez, J. L.: Field Delopyable, High-Resolution, Time-of-Flight Aerosol Mass Spectrometer, Anal. Chem., 78, 8281-8289, 2006.
16. Durdina, L., Lobo, P., Trueblood, M.B., Black, E.A., Achterberg, S., Hagen, D., Brem, B.T., and Wang, J.: Response of black carbon-mass instruments to mini-cast soot, Aerosol Sci. Technol., 50, 906-918, 2016.
17. Dusek, U., Frank, G. P., Hildebrandt, L., Curtius, J., Schneider, J., Walter, S., Chand, D., Drewnick, F., Hings, S., Jung, D., Borrmann, S., and Andreae, M. O.: Size matters more than chemistry for cloud-nucleating ability of aerosol particles, Science, 312, 1375–1378, 2006.
18. Ervens, B., Cubison, M., Andrews, E., Feingold, G., Ogren, J. A., Jimenez, J. L., DeCarlo, P., and Nenes, A.: Prediction of cloud condensation nucleus number concentration using measurements of aerosol size distributions and composition and light scattering enhancement due to humidity, J. Geophys. Res., 112, doi:10.1029/2006JD007426, 2007.

19. Farmer, D. K., Cappa, C. D., & Kreidenweis, S.: Atmospheric processes and their controlling influence on cloud condensation nuclei activity." Chemical Reviews 115.10, 4199-4217, 2015. doi.org/10.1021/cr5006292
20. Fofie, E. A., N. M. Donahue, and Asa-Awuku, A.: Cloud condensation nuclei activity and droplet formation of primary and secondary organic aerosol mixtures, Aerosol Sci. Technol., 52, 1-10, 2017.
21. Gibson, E. R., Gierlus, K. M., Hudson, P. K., and Grassian, V. H.: Generation of Internally Mixed Insoluble and Soluble Aerosol Particles to Investigate the Impact of Atmospheric Aging and Heterogeneous Processing on the CCN Activity of Mineral Dust Aerosol, Aerosol Sci. Technol., 41, 914-924, doi: 10.1080/02786820701557222, 2007.
22. Hameri , K. , Charlson , R. and Hansson , H. C.: Hygroscopic Properties of Mixed Ammonium Sulfate and Carboxylic Acids Particles, AIChE J., 48, 1309–1316, 2002.
23. Henning, S., Rosenørn, T., D'Anna, B., Gola, A. A., Svenningsson, B., and Bilde, M.: Cloud droplet activation and surface tension of mixtures of slightly soluble organics and inorganic salt, Atmos. Chem. Phys., 5, 575-582, doi:10.5194/acp-5-575-2005, 2005.
24. Jurányi, Z., Tritscher, T., Gysel, M., Laborde, M., Gomes, L., Roberts, G., Baltensperger, U. and Weingartner, E.: Hygroscopic mixing state of urban aerosol derived from size-resolved cloud condensation nuclei measurements during the MEGAPOLI campaign in Paris, Atmos. Chem. Phys., 13(13), 6431–6446, 2013.
25. Kim, N., Park, M., Yum, S. S., Park, J. S., Shin, H. J. and Ahn, J. Y.: Impact of urban aerosol properties on cloud condensation nuclei (CCN) activity during the KORUS-AQ field campaign, Atmos. Environ., 185, 221–236, 2018.
26. King, S. M., Rosenoern, T., Shilling, J. E., Chen, Q. and Martin, S. T.: Cloud condensation nucleus activity of secondary organic aerosol particles mixed with sulfate, Geophys. Res. Lett., 34(24), 3589, 2007.
27. Koehler, K. A., DeMott, P. J., Kreidenweis, S. M., Popovicheva, O. B., Petters, M. D., Carrico, C. M., Kireeva, E. D., Khokhlova, T. D. and Shonija, N. K.: Cloud condensation nuclei and ice nucleation activity of hydrophobic and hydrophilic soot particles, Phys. Chem. Chem. Phys., 11(36), 7906–7920, 2009.
28. Kuwata, M. and Kondo, Y.: Dependence of size-resolved CCN spectra on the mixing state of nonvolatile cores observed in Tokyo. J. Geophys. Res. 113, D19202, 2008.
29. Lammel, G. and Novakov, T.: Water Nucleation Properties of Carbon-Black and Diesel Soot Particles, Atmos. Environ., 29(7), 813–823, 1995.

30. Lance, S., Raatikainen, T., Onasch, T., Worsnop, D. R., Yu, X.Y., Alexander, M. L., Stolzenburg, M. R., McMurry, P. H., Smith, J. N., and Nenes, A.: Aerosol mixing-state, hygroscopic growth and cloud activation efficiency during MIRAGE 2006, Atmos. Chem. Phys. Discuss., 12, 15709–15742, doi:10.5194/acpd-12-15709-2012, 2012.
31. Lance, S., Onasch, T., Warsnop, D., Yu, X. Y., Alexander, L., Stolzenberg, M., McMurry, P., Smith, J.N., Nenes., A.: Aerosol Mixing-State and Cloud Activation Efficiency during the MILAGRO Campaign, 2013, Atmos. Chem. Phys., 13, 5049-5062, doi:10.5194/acp-13-5049-2013, 2013.
32. Liu, D., Allan, J., Whitehead, J., Young, D., Flynn, M., Coe, H., McFiggans, G., Fleming, Z. L., and Bandy, B.: Ambient black carbon particle hygroscopic properties controlled by mixing state and composition, Atmos. Chem. Phys., 13, 2015-2029, doi:10.5194/acp-13-2015-2013, 2013.
33. Mahish, M., Jefferson, A. and Collins, D. R.: Influence of Common Assumptions Regarding Aerosol Composition and Mixing State on Predicted CCN Concentration, Atmosphere , 9(2), 54, 2018.
34. Mallet, M. D., Cravigan, L. T., Milic, A., Alroe, J., Ristovski, Z. D., Ward, J., Keywood, M., Williams, L. R., Selleck, P. and Miljevic, B.: Composition, size and cloud condensation nuclei activity of biomass burning aerosol from northern Australian savannah fires, Atmos. Chem. Phys., 17(5), 3605–3617, 2017.
35. Mamakos, A., Khalek, I., Giannelli, R. and Spears, M.: Characterization of Combustion Aerosol Produced by a Mini-CAST and Treated in a Catalytic Stripper, Aerosol Science and Technology, 47(8), 927–936, doi:10.1080/02786826.2013.802762, 2013.
36. Maricq, M. M. and Matti Maricq, M.: Examining the Relationship Between Black Carbon and Soot in Flames and Engine Exhaust, Aerosol Science and Technology, 48(6), 620–629, doi:10.1080/02786826.2014.904961, 2014.
37. McMeeking, G. R., Good, N., Petters, M. D., McFiggans, G. and Coe, H.: Influences on the fraction of hydrophobic and hydrophilic black carbon in the atmosphere, Atmos. Chem. Phys., 11(10), 5099–5112, 2011.
38. Meng, J. W., Yeung, M. C., Li, Y. J., Lee, B. Y. L. and Chan, C. K.: Size-resolved cloud condensation nuclei (CCN) activity and closure analysis at the HKUST Supersite in Hong Kong, Atmos. Chem. Phys., 14(18), 10267–10282, 2014.
39. Moore, R. H., Nenes., A. and Medina., J.: Scanning Mobility CCN Analysis - A Method for Fast Measurements of Size-Resolved CCN Distributions and Activation Kinetics, Aerosol Sci. Technol., 44, 861-871, 2010.

40. Moore, R. H., Cerully, K., Bahreini, R., Brock, C. A., Middlebrook, A. M. and Nenes, A.: Hygroscopicity and composition of California CCN during summer 2010, J. Geophys. Res., 117, D00V12, doi:10.1029/2011JD017352, 2012.
41. Moore, R. H., Raatikainen, T., Langridge, J. M., Bahreini, R., Brock, C. A., Holloway, J. S., Lack, D. A., Middlebrook A. M., Perring, A. E., Schwarz, J. P., Spackman, J. R., and Nenes, A.: CCN Spectra, Hygroscopicity, and Droplet Activation Kinetics of Secondary Organic Aerosol Resulting from the 2010 Deepwater Horizon Oil Spill, Env. Sci. Tech., 26, 3093-3100, 2012.
42. Moore, R. H., Ziemba, L. D., Dutcher, D., Beyersdorf, A. J., Chan, K., Crumeyrolle, S., Raymond, T. M., Thornhill, K. L., Winstead, E. L. and Anderson, B. E.: Mapping the Operation of the Miniature Combustion Aerosol Standard (Mini-CAST) Soot Generator, Aerosol Science and Technology, 48(5), 467–479, doi:10.1080/02786826.2014.890694, 2014.
43. Padró, L. T., Asa-Awuku, A., Morrison, R., and Nenes, A.: Inferring thermodynamic properties from CCN activation experiments: single-component and binary aerosols, Atmos. Chem. Phys., 7, 5263-5274, doi:10.5194/acp-7-5263-2007, 2007.
44. Padró, L. T., Moore, R. H., Zhang, X., Rastogi, N., Weber, R. J., and Nenes, A.: Mixing state and compositional effects on CCN activity and droplet growth kinetics of size-resolved CCN in an urban environment, Atmos. Chem. Phys., 12, 10239-10255, doi:10.5194/acp-12-10239-2012, 2012.
45. Paramonov, M., Aalto, P. P., Asmi, A., Prisle, N., Kerminen, V.-M., Kulmala, M. and Petäjä, T.: The analysis of size-segregated cloud condensation nuclei counter (CCNC) data and its implications for cloud droplet activation, Atmos. Chem. Phys., 13(20), 10285–10301, 2013.
46. Petters, M. D. and Kreidenweis, S. M.: A single parameter representation of hygroscopic growth and cloud condensation nucleus activity – Part 2: Including solubility, Atmos. Chem. Phys., 8, 6273-6279, doi:10.5194/acp-8-6273-2008, 2008.
47. Petters, M. D. and Kreidenweis, S. M.: A single parameter representation of hygroscopic growth and cloud condensation nucleus activity, Atmos. Chem. Phys., 7, 1961-1971, doi:10.5194/acp-7-1961-2007, 2007.
48. Pruppacher, H. R. and Klett, J. D.: Microphysics of Clouds and Precipitation, 954, Kluwar Acad., Norwell Mass., 1997.

570 49. Pinho, C. E. L., João M P, Ferreira, V., Pilão, R. and Pinho, C.: Influence of Burner Geometry on Flame
571 Characteristics of Propane-Air Mixture: Experimental and Numerical Studies, Defect and Diffusion Forum,
572 273-276, 162–167, doi:10.4028/www.scientific.net/ddf.273-276.162, 2008.
573 50. Riemer, N., Ault, A. P., West, M., Craig, R. L. and Curtis, J. H.: Aerosol Mixing State: Measurements,
574 Modeling, and Impacts, Reviews of Geophysics, doi:10.1029/2018rg000615, 2019.
575 51. Rojas, L., Peraza, A. and Ruette, F.: Aging Oxidation Reactions on Atmospheric Black Carbon by OH Radicals.
576 A Theoretical Modeling Study, J. Phys. Chem. A, 119(52), 13038–13047, 2015
577 52. Roberts, G. C. and Nenes, A.: A Continuous-Flow Streamwise Thermal-Gradient CCN Chamber for
578 Atmospheric Measurements, Aerosol Sci. Technol., 35, 206-2011, doi: 10.1080/027868290913988, 2005.
579 53. Rose, D., Gunthe, S. S., Mikhailov, E., Frank, G. P., Dusek, U., Andreae, M. O., Poschl, U.: Calibration and
580 measurement uncertainties of a continuous-flow cloud condensdation nuclei counter (DMT-CCNC): CCN
581 Activation of ammonium sulfate and sodium chloride aerosol particles in theory and experiment, Atmos. Chem.
582 Phys., 8, 1153-1179, doi: 10.5194/acp-8-1153-2008, 2008.
583 54. Sánchez Gácita, M., Longo, K. M., Freire, J. L. M., Freitas, S. R. and Martin, S. T.: Impact of mixing state and
584 hygroscopicity on CCN activity of biomass burning aerosol in Amazonia, Atmos. Chem. Phys., 17(3), 2373-
585 2392, 2017.
586 55. Saxena, P., Hildemannm, L. M.: Water-Soluble organics in atmospheric particles: A critical review of the
587 litereature and application of thermodynamics to identify candidate compounds, J. Atmos. Chem., 24, 57-109,
588 1996.
589 56. Sánchez Gácita, M., Longo, K. M., Freire, J. L. M., Freitas, S. R. and Martin, S. T.: Impact of mixing state and
590 hygroscopicity on CCN activity of biomass burning aerosol in Amazonia, Atmos. Chem. Phys., 17(3), 2373-
591 2392, 2017.
592 57. Seinfeld, J. H. and Pandis, S. N.: Atmopsheric Chemistry and Physics, John Wiley, New York, 1998.
593 58. Seong, H. J. and Boehman, A. L.: Studies of soot oxidative reactivity using a diffusion flame burner,
594 Combustion and Flame, 159(5), 1864–1875, doi:10.1016/j.combustflame.2012.01.009, 2012.
595 59. Shulman, M. L., Jacobson, M. C., Charlson, R. J., Synovec, R. E., and Young, T. E.: Dissolution behavior and
596 surface tension effects of organic compounds in nucleating cloud droplets, Geophys. Res. Lett., 23, 277–280,
597 1996.

60. Su, H., Rose, D., Cheng, Y. F., Gunthe, S. S., Massling, A., Stock, M., Wiedensohler, A., Andreae, M. O., and Poschl, U.: Hygroscopicity distribution concept for measurement data analysis and modeling of aerosol particle mixing state with regard to hygroscopic growth and CCN activation. Atmos. Chem. Phys., 10, 7489-7503, 2010.
61. Spracklen, D. V., Carslaw, K. S., Poschl, U., Rap, A. and Forster, P. M.: Global cloud condensation nuclei influenced by carbonaceous combustion aerosol, Atmos. Chem. Phys., 11(17), 9067–9087, 2011.
62. Stevens, R. and Dastoor, A.: A Review of the Representation of Aerosol Mixing State in Atmospheric Models, Atmosphere , 10(4), 168, 2019.
63. Sullivan R. C., Moore M., Petters, M. D., Kreidenweis S. M., Roberts G. C., and Prather, K. A.: Effect of chemical mixing state on the hygroscopicty and cloud nucleating properties of calcium mineral dust particles, Atmos. Chem. Phys., 9, 3303-3316, 2009.
64. Svenningsson, B., Rissler, J., Swietlicki, E., Mircea, M., Bilde, M., Facchini, M. C., Decesari, S., Fuzzi, S., Zhou, J., Mønster, J., and Rosenørn, T.: Hygroscopic growth and critical supersaturations for mixed aerosol particles of inorganic and organic compounds of atmospheric relevance, Atmos. Chem. Phys., 6, 1937-1952, doi:10.5194/acp-6-1937-2006, 2006.
65. Vu, D., Short, D., Karavalakis, G., Durbin, T. D., and Asa-Awuku, A.: Integrating cloud condensation nuclei predictions with fast time resolved aerosol instrumentation to determine the hygroscopic properties of emissions over transient drive cycles, Aerosol Sci. Technol., 49, 1149-1159, 2015.
66. Wang, J., Cubison, M. J., Aiken, A. C., Jimenez, J. L. and Collins, D. R.: The importance of aerosol mixing state and size-resolved composition on CCN concentration and the variation of the importance with atmospheric aging of aerosols, Atmos. Chem. Phys., 10(15), 7267–7283, 2010.
67. Weingartner, E., Burtscher, H. and Baltensperger, U.: Hygroscopic properties of carbon and diesel soot particles, Atmospheric Environment, 31(15), 2311–2327, doi:10.1016/s1352-2310(97)00023-x, 1997.
68. Wex, H., McFiggans, G., Henning, S., and Stratmann, F.: Influence of the external mixing state of atmospheric aerosol on derived CCN number concentrations, Geophys. Res. Lett., 37, doi:10.1029/2010GL043337, 2010.
69. Winkler, P.: The growth of atmospheric aerosol particles as a function of the relative humidity—II. An improved concept of mixed nuclei, J. Aerosol Sci., 4(5), 373–387, 1973.

70. Ye, Q., Robinson, E. S., Ding, X., Ye, P., Sullivan, R., and Robinson, N.: Mixing of secondary organic aerosols versus relative humidity, Proc. Natl. Acad. Sci. U. S. A., 113, 12649-12654, 2016.

71. Zaveri, R. A., Barnard, J. C., Easter, R. C., Riemer, N. and West, M.: Particle-resolved simulation of aerosol size, composition, mixing state, and the associated optical and cloud condensation nuclei activation properties in an evolving urban plume, J. Geophys. Res. D: Atmos., 115(D17) [online] Available from: https://onlinelibrary.wiley.com/doi/pdf/10.1029/2009JD013616, 2010.

Figures for:

External and Internal CCN Mixtures: Controlled Laboratory Studies of Varying Mixing States

Diep Vu, Shaokai Gao, Tyler Berte, Mary Kacarab, Qi Yao[4], Kambiz Vafai and Akua Asa-Awuku*

Number of Pages: 14

Number of Figures: 9

Number of Appendix Figures: 2

* Corresponding Author.

E-mail address: asaawku@umd.edu (A. Asa-Awuku)

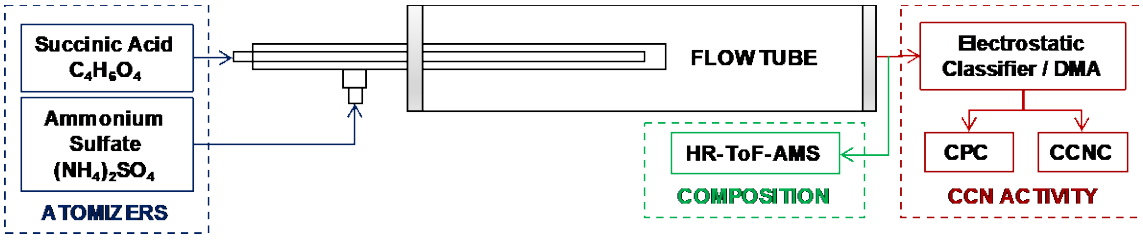
Succinic Acid
$C_4H_6O_4$
Ammonium Sulfate
$(NH_4)_2SO_4$
ATOMIZERS
FLOW TUBE
HR-ToF-AMS
COMPOSITION
Electrostatic Classifier / DMA
CPC
CCNC
CCN ACTIVITY

fig01

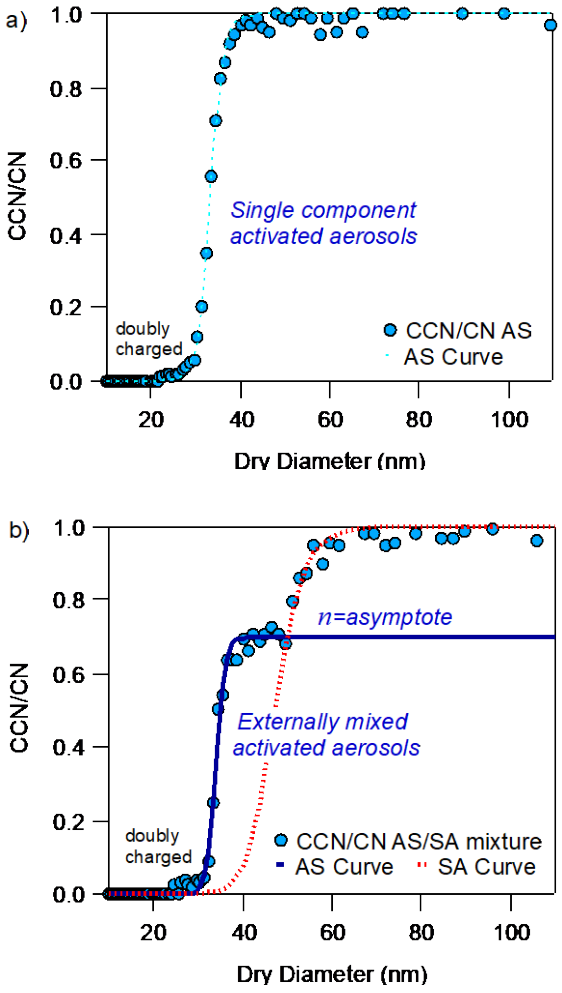
a)
1.0
0.8
0.6
0.4
0.2
0.0
CCN/CN
Single component
activated aerosols
doubly
charged
CCN/CN AS
AS Curve
20
40
60
80
100
Dry Diameter (nm)
b)
1.0
0.8
0.6
0.4
0.2
0.0
CCN/CN
n=asymptote
Externally mixed
activated aerosols
doubly
charged
CCN/CN AS/SA mixture
AS Curve
SA Curve
20
40
60
80
100
Dry Diameter (nm)

fig02

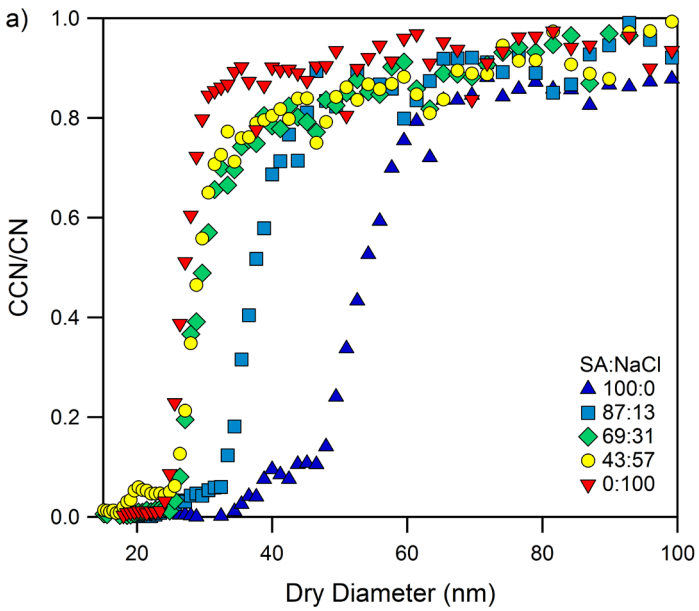
a)
CCN/CN
Dry Diameter (nm)
SA:NaCl
100:0
87:13
69:31
43:57
0:100

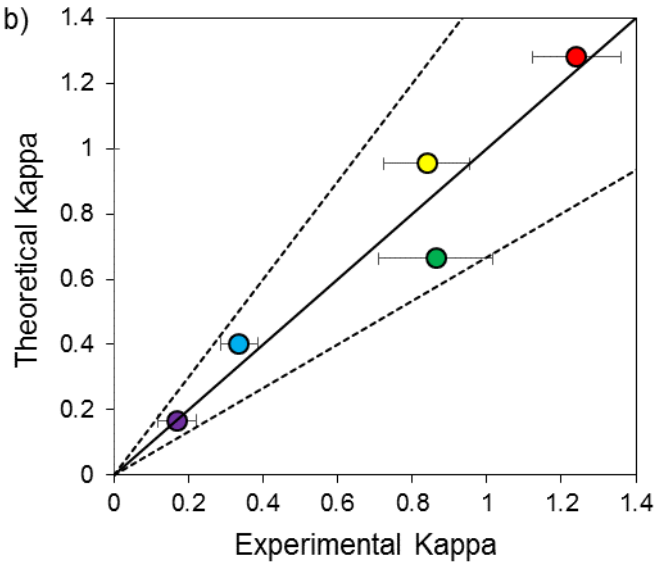
b)
Theoretical Kappa
Experimental Kappa

fig03

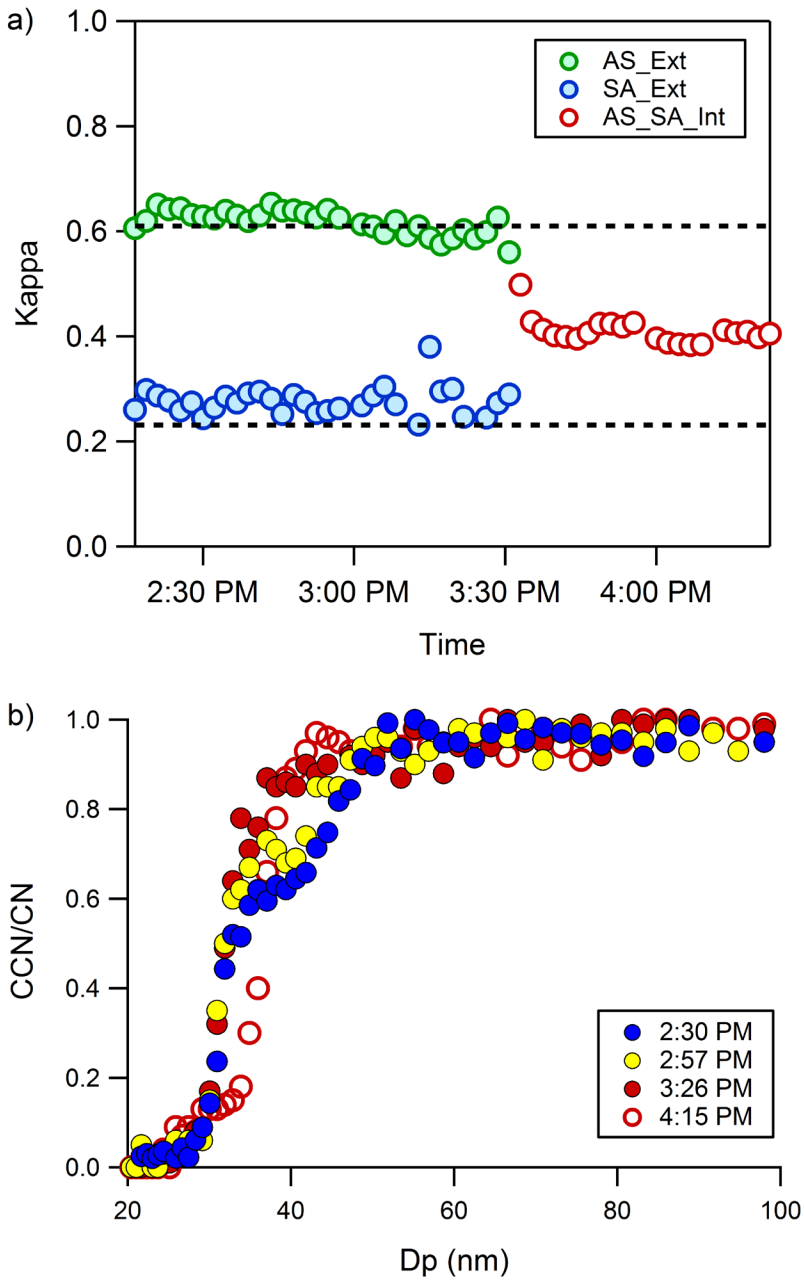
a)
1.0
0.8
0.6
0.4
0.2
0.0
Kappa
AS_Ext
SA_Ext
AS_SA_Int
2:30 PM
3:00 PM
3:30 PM
4:00 PM
Time
b)
1.0
0.8
0.6
0.4
0.2
0.0
CCN/CN
2:30 PM
2:57 PM
3:26 PM
4:15 PM
20
40
60
80
100
Dp (nm)

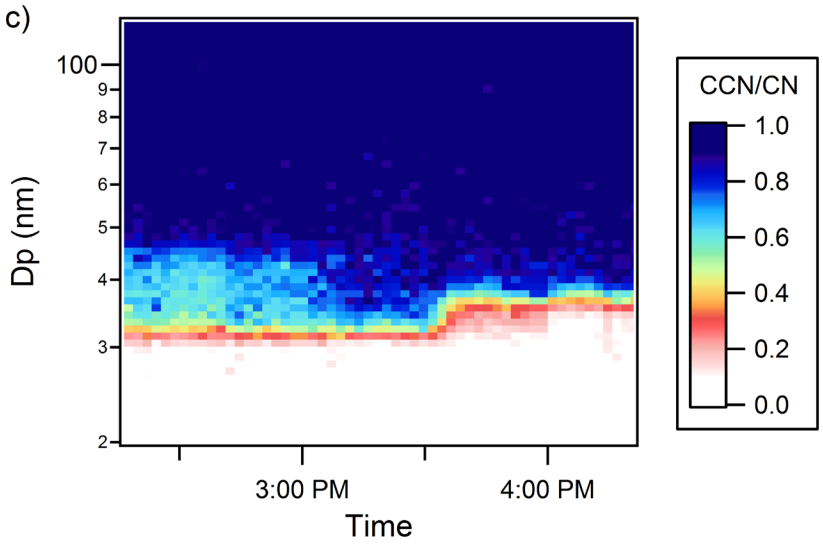

fig04

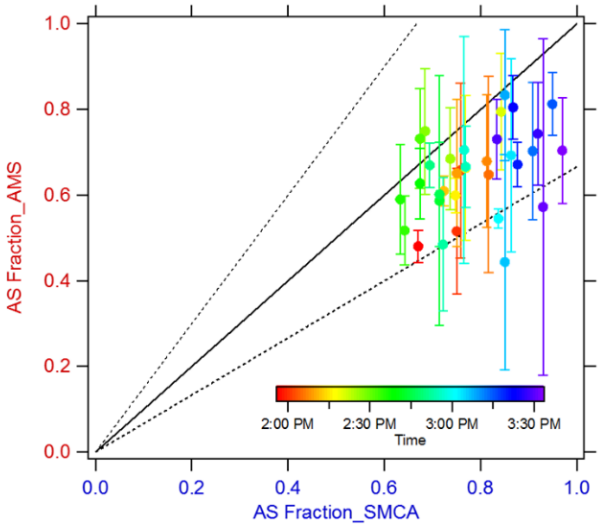
AS Fraction_AMS
AS Fraction_SMCA
0.0
0.2
0.4
0.6
0.8
1.0
2:00 PM
2:30 PM
3:00 PM
3:30 PM
Time

Fig05

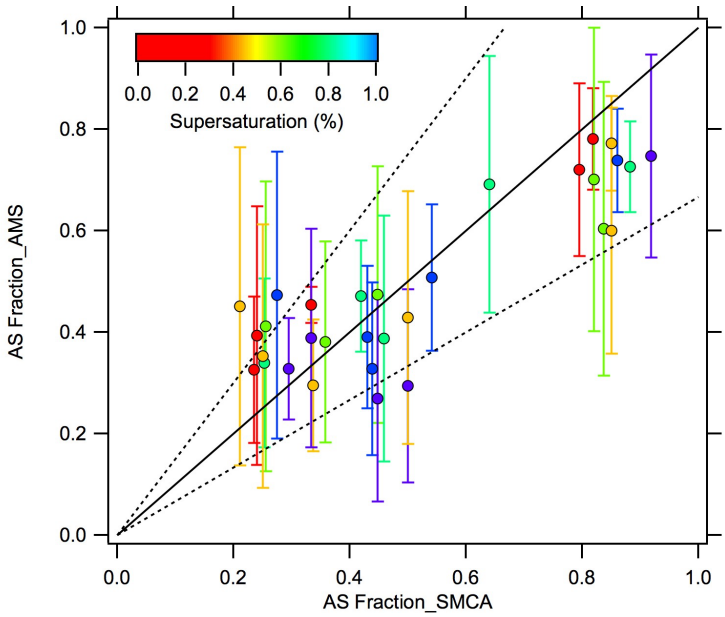
0.0 0.2 0.4 0.6 0.8 1.0
Supersaturation (%)
AS Fraction_AMS
AS Fraction_SMCA
0.0
0.2
0.4
0.6
0.8
1.0

fig06

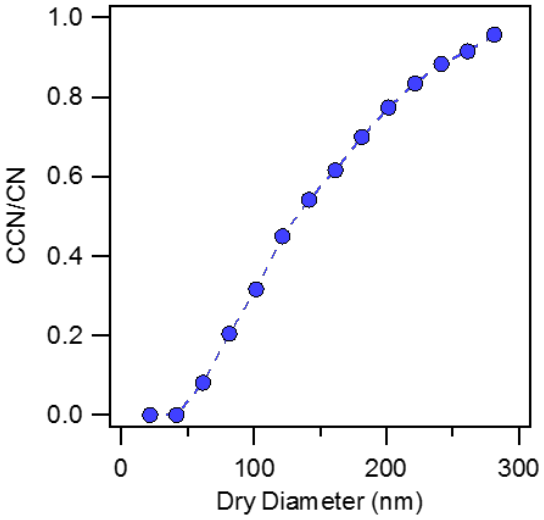

fig07

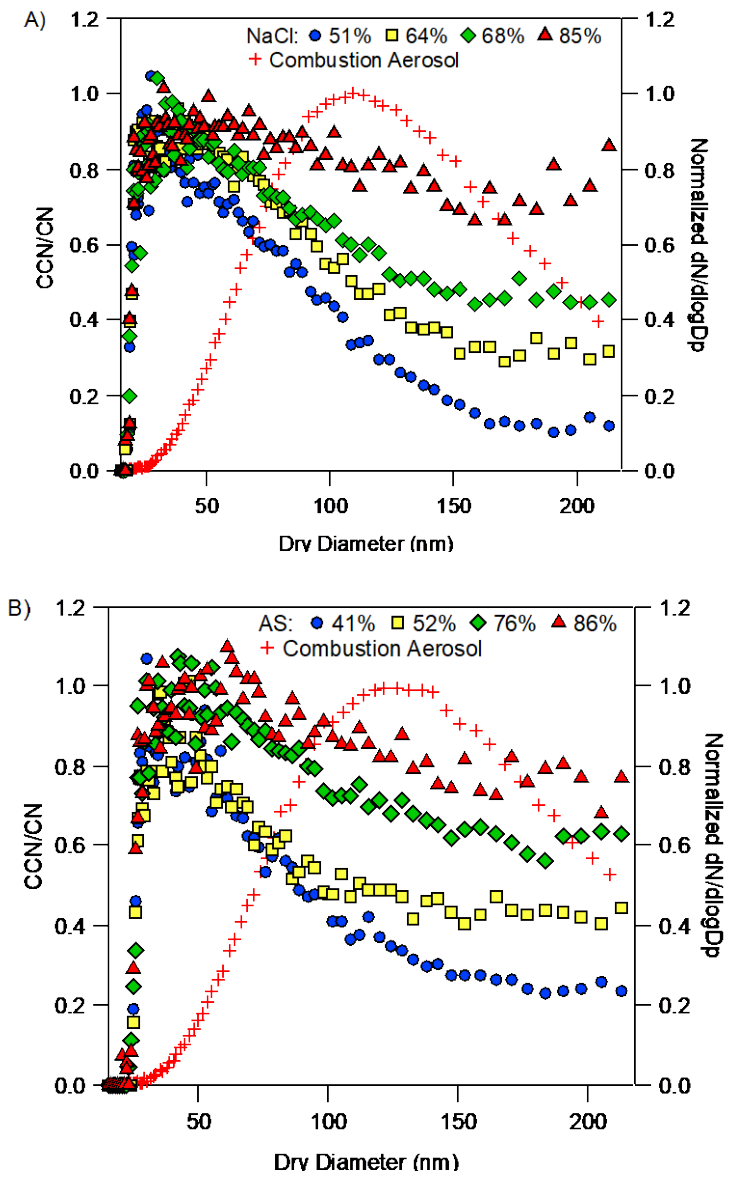
A)
NaCl: 51% 64% 68% 85%
Combustion Aerosol
CCN/CN
Normalized dN/dlogDp
Dry Diameter (nm)
B)
AS: 41% 52% 76% 86%
Combustion Aerosol
CCN/CN
Normalized dN/dlogDp
Dry Diameter (nm)

fig08

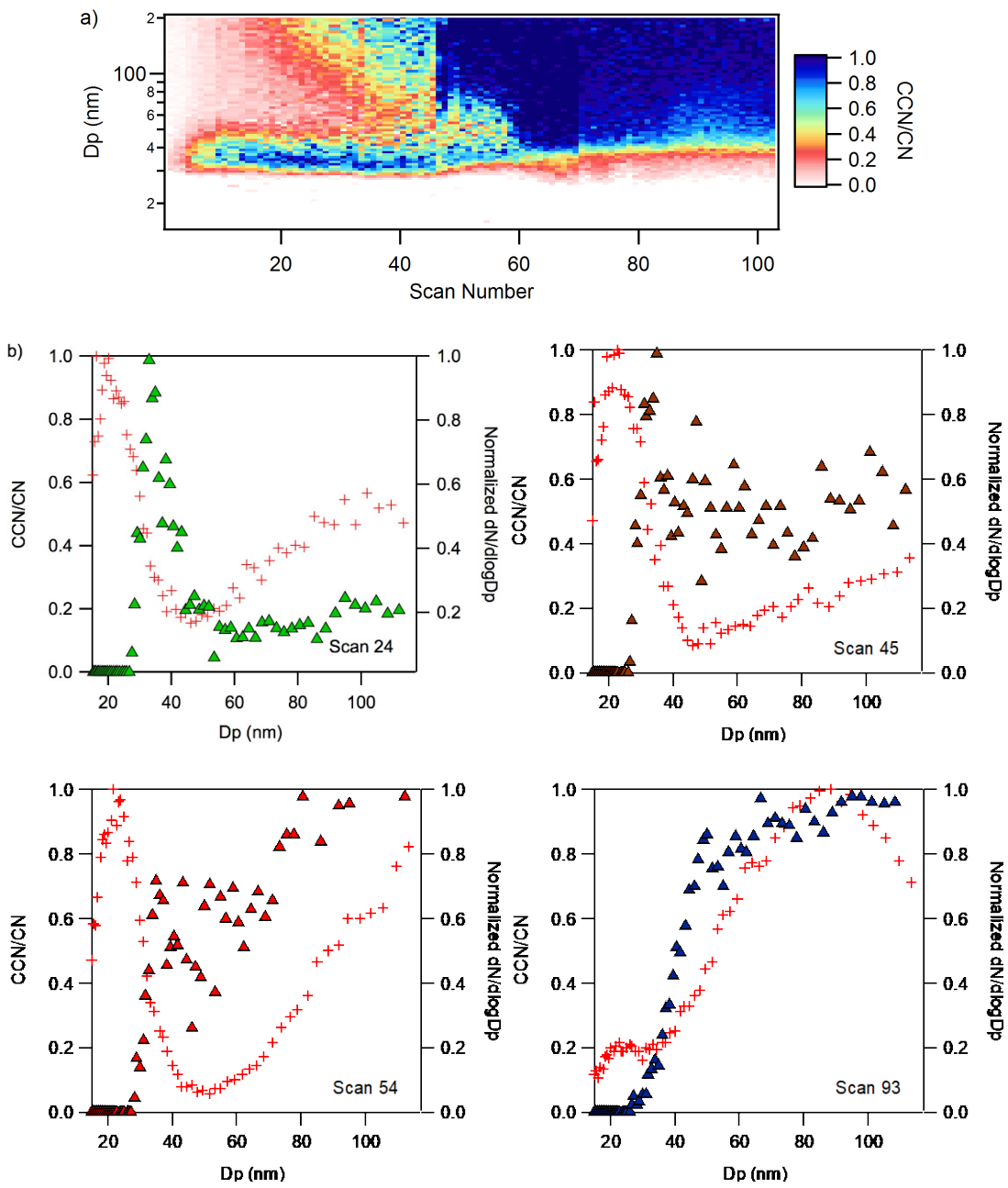
a)
Dp (nm)
Scan Number
CCN/CN
b)
Scan 24
Scan 45
Scan 54
Scan 93
Dp (nm)
CCN/CN
Normalized dN/dlogDp

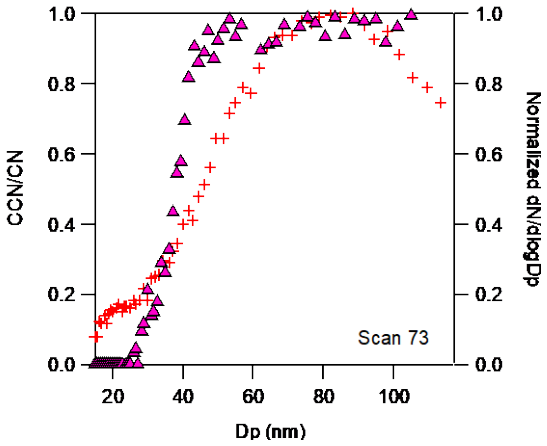
CCN/CN
Normalized dN/dlogDp
Dp (nm)
Scan 73
1.0
0.8
0.6
0.4
0.2
0.0
20
40
60
80
100

Fig09